

## A Snowflake Divertor: a Possible Way of Improving the Power Handling in Future Fusion Facilities

D.D. Ryutov<sup>1</sup>, R.H. Bulmer<sup>1</sup>, R.H. Cohen<sup>1</sup>, D.N. Hill<sup>1</sup>, L. Lao<sup>2</sup>, J.E. Menard<sup>3</sup>, T.W. Petrie<sup>2</sup>,  
L.D. Pearlstein<sup>1</sup>, T.D. Rognlien<sup>1</sup>, P.B. Snyder<sup>2</sup>, V. Soukhanovskii<sup>1</sup>, M.V. Umansky<sup>1</sup>

<sup>1</sup> Lawrence Livermore National Laboratory, Livermore, CA 94551, USA

<sup>2</sup> General Atomics, San Diego, CA 92186, USA

<sup>3</sup> Princeton Plasma Physics Laboratory, Princeton, NJ 08543, USA

### Abstract

Handling high power loads on plasma facing components is one of the critical issues in developing an economically competitive fusion reactor or fusion test facilities based on a tokamak. In this study, we provide a detailed analysis of a relatively unexplored approach to this problem based on the use of divertors with the poloidal magnetic field structure closely approaching a second-order null. We demonstrate that this geometry opens up new possibilities for radiative divertors, has favorable effect on the plasma transport, and provides an additional control over ELM activity. In the ideal case where the null is exactly second order, the separatrix near the null acquires a characteristic hexagonal shape reminiscent of a snowflake, whence the name of this configuration. It can be created by a simple set of divertor coils situated outside the toroidal field coils.

### 1. Introduction

Handling high power loads on plasma facing components is one of the critical issues in developing an economically competitive fusion reactor or fusion test facilities based on tokamak. The optimal choice of a heat-load mitigation problem for a given device will be made based on a variety of considerations, including details of plasma equilibrium, life-time and maintainability of in-vessel components, the complexity of the magnetic system, and many others. The decision can be made only on the basis of an integrated design, which is still in the future. So, parallel research into several approaches seems quite reasonable now.

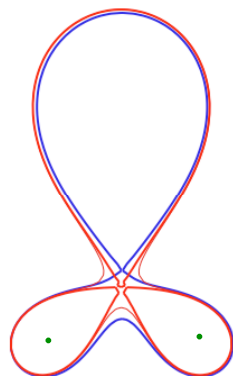


*Fig. 1 Separatrix for the exact second-order null (thick red line) and the nearby flux surface (thin red line). Separatrix for the snowflake-plus configuration is shown in blue. The divertor coils are shown in green dots.*

In this paper we consider the “snowflake” (“SF”) divertor configuration, first described in Refs. [1, 2]. This divertor exploits a tokamak geometry in which the poloidal magnetic field null approaches second order; the name stems from the characteristic hexagonal, snowflake-like, shape of the separatrix for an exact second-order null (Fig. 1). The poloidal magnetic field in this case is a

quadratic function of the distance to the null, whereas in the standard X-point configuration it is a linear function. This means that the flux expansion is much larger in the vicinity of a null of a snowflake divertor, and one can try to exploit this fact for reducing the divertor heat load.

When using the terms “X-point divertor” or “standard X-point configuration”, we mean a configuration with an X-shaped separatrix near the null point. This should not be confused with the recently proposed “X-divertor,” where additional coils cause significant reduction of the magnetic field in the divertor legs at some distance from the X-point [3], and the even more recent “super-X divertor” [4], where further reduction of the heat load is expected to occur due to a significant increase of the major radius and thus available surface area in the outer strike-point region.

The SF configuration can be created by a simple set of divertor (poloidal field) coils (an example is shown in Fig. 1), having currents  $I_d$  related in a certain way to the plasma current [1]. The distance from the divertor coils to the null-point is approximately equal to the plasma minor radius. For large facilities, this allows placing divertor coils outside toroidal field coils.

Typically, the current  $I_{d0}$  that makes an exact second-order null is of order of the plasma current  $I_p$ . If the current in the divertor coils is higher than  $I_{d0}$ , the configuration becomes an X-point configuration, but with a small gradient of the poloidal field near the null-point. We call this configuration a “snowflake-plus” (Fig. 1, blue line). Its advantage is that it is remarkably robust with respect to possible un-controlled variations of the plasma current [1,2]. For a current  $I_d$  that is lower than  $I_{d0}$ , two X-points appear on the separatrix. We call it a “snowflake-minus” configuration [1,2]. Our main emphasis here is on the snowflake-plus configuration.

## 2. General properties of a snowflake configuration

In Ref. [1] it was pointed out that exact snowflake configuration is topologically unstable, and that it might be beneficial to operate the divertor in the aforementioned “snowflake-plus” mode, where the current  $I_d$  in divertor coils is somewhat higher than the one that corresponds to an exact snowflake configuration. In this case, if the configuration remains symmetric with respect to the  $x=0$  plane, the expansion of the flux function near the null point acquires the form:

$$\Phi = \frac{I}{c} \left[ \eta z + \frac{A}{r_e^2} \left( x^2 z - \frac{z^3}{3} \right) \right] + C, \quad (1)$$

where  $x$  and  $z$  are horizontal and vertical coordinates in the poloidal plane of Fig. 1,  $r_e$  is the distance between the magnetic axis and the separatrix in the equatorial plane (roughly, the plasma minor radius), the constant  $A$  of order unity depends on details of the geometry of PF coils, and constant  $\eta$  characterizes the proximity to an exact snowflake. In the simple model shown in Fig. 1 it is merely

$$\eta \equiv (I_d - I_{d0}) / I_{d0}. \quad (2)$$

The constant  $C$  is determined by the condition that the poloidal magnetic flux be zero ( $\Phi=0$ ) on the separatrix. In the exact snowflake configuration this constant is zero.

The distance between some magnetic surface and the separatrix near the magnetic field null increases significantly compared to that distance in the equatorial plane of the device. A key characteristic of this flaring effect is the minimum distance between the null-point and a magnetic surface,  $\Delta_0$ , compared to the distance  $\Delta_e$  between this magnetic surface and the separatrix near the equatorial plane. The larger the ratio

$$F \equiv \Delta_0 / \Delta_e, \quad (3)$$

the stronger the flaring. Another way of characterizing the flux expansion is comparing the minimum of the poloidal magnetic field on a certain flux surface,  $B_{pmin}$ , to the value of the poloidal field in the equatorial plane,  $B_{pe}$ . The corresponding ratio is denoted by  $G \equiv B_{pe} / B_{pmin}$ . Both  $F$  and  $G$  are presented in Fig. 2 for the snowflake divertor ( $S$  subscript) and the standard X-point divertor ( $X$  subscript), for a similar overall plasma shape. One sees that, indeed, the SF configuration provides significantly stronger flux expansion than the standard one.

Another benefit of the snowflake geometry is related by its effect on the magnetic shear just *inside* the separatrix, in the pedestal region. We define the magnetic shear in the vicinity of the separatrix as

$$S = r_e dq / d\Delta_e, \quad (4)$$

where  $q$  is a standard safety factor, and  $\Delta_e$  is defined before Eq. (3). The magnetic shear is shown in Fig. 3. One sees that, by a mere 5% variation of the current in the divertor coils, one can significantly change the shear in the pedestal region. This may provide a useful tool for the control over the peeling-ballooning instability that is thought to play a significant role in the behavior of ELMs [5,6].

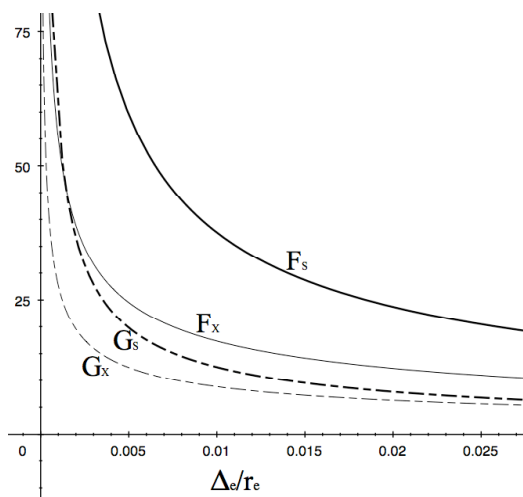


Fig. 2 Geometrical expansion parameters for a snowflake (bold line) and X-point configurations (thin line). The parameter  $r_e$  is the distance from the magnetic axis to the separatrix in the equatorial plane. At the boundary of a typical SOL, one has  $\Delta_e/r_e \sim 0.01 - 0.003$ , so that the ratio  $F_s/F_x$  is in the range of 1.5-3. Dashed lines represent the magnetic expansion parameter  $G$ . The ratio  $G_s/G_x$  is in the range 1.5-2.

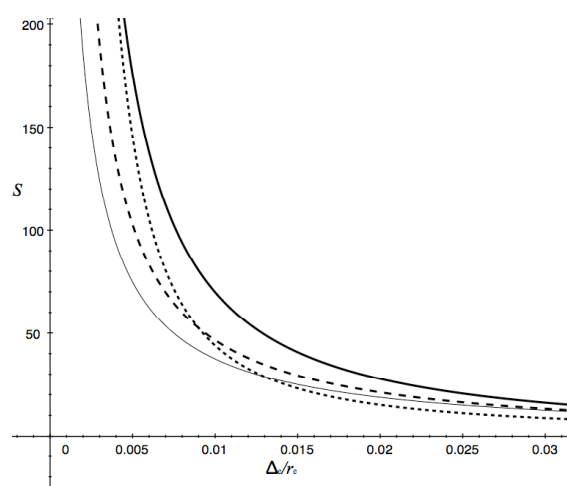


Fig. 3 Magnetic shear for the standard X-point divertor, thin line, and for the snowflake-plus divertor, thick lines. Solid line:  $\eta=0$  (an exact snowflake); dashed line:  $\eta=0.025$ ; dotted line:  $\eta=0.05$ . Large values of the parameter  $S$  are related to the normalization. More important is the change of the  $S$  profile for the snowflake divertor compared to that of a standard divertor: in the immediate vicinity of the separatrix, the snowflake-plus divertor yields higher value of  $S$ , whereas at some distance from the separatrix, deeper into the pedestal region,  $S$  can become both larger and smaller than for the X-point divertor. This can be used to control ELM activity.

The magnetic shear outside the separatrix causes a stronger squeezing of the magnetic flux tubes passing near the magnetic null point than for the standard divertor. The shear will have a strong effect on the SOL turbulence (see Sec. 5 below).

### 3. Snowflake in specific devices

In some cases, the snowflake configuration can be created on existing devices, with the use of only existing poloidal field coils. We have looked into this possibility for the DIII-D tokamak at General Atomics. Figure 4 shows the CORSICA [7] magnetic-equilibrium solution for a shot with a plasma current of 1 MA. This figure corresponds to the parameter  $\eta \sim 0.03$ . Importantly, the plasma current in each PF coil does not exceed its coil current-carrying capacity.

The snowflake geometry is also compatible with spherical tori. Figure 5 shows a possible snow-flake-plus configuration for the proposed high-heat-flux facility at PPPL [8]. Figure 6 shows the transition from the snowflake-plus to the snowflake-minus geometry with the NSTX spherical torus. The change from SF-plus to SF-minus configuration required only

10% change in the current distribution between PF coils. Figures 5, 6 were obtained based on the ISOLVER code [9].

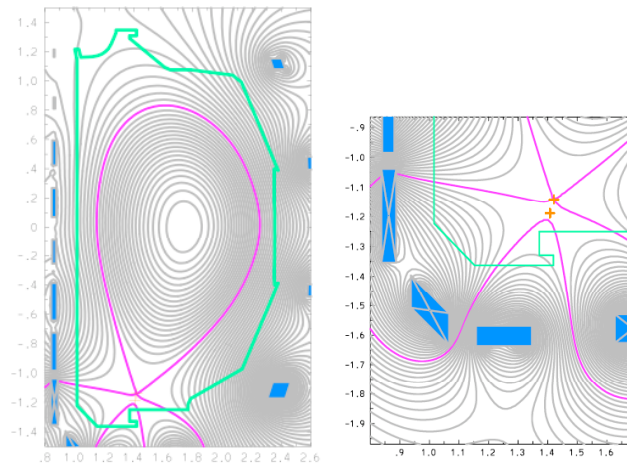


Fig. 4. Snowflake configuration for the DIII-D tokamak. Left panel: general view of the poloidal cross-section; right panel: blow-up of the divertor region. Shown in blue are poloidal field coils; separatrix is shown in pink. Plasma current is 1 MA. The configuration corresponds to the snowflake-plus geometry with the parameter  $\eta \sim 0.03$ .

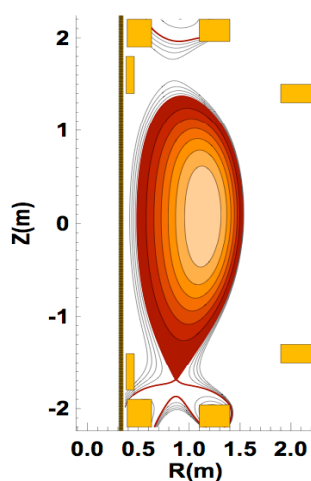


Fig. 5 A snowflake-plus configuration for the proposed high-heat-flux spherical torus NHTX (PPPL).

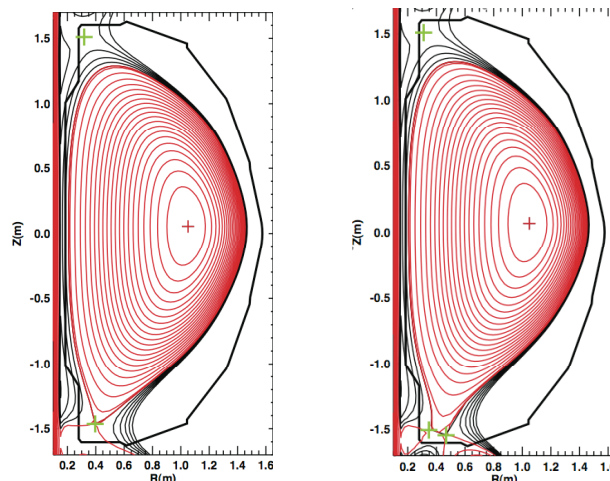


Fig. 6 Snowflake-plus (left panel) and snowflake-minus (right panel) configurations for the NSTX spherical torus (PPPL). Note the appearance of two closely spaced nulls in the second case (light-green crosses).

#### 4. First UEDGE plasma transport simulations.

The Fusion Development Facility (FDF) [10], aimed at neutron and other testing of the reactor components, will have to handle high heat fluxes in the divertor. We have applied the UEDGE code [11] to assess possible benefits of the snowflake geometry for the anticipated parameters for the FDF facility. Figure 7 shows the comparison of the magnetic field structure for the X-point geometry (left panel) and snowflake-plus geometry (right panel). Note that the shape of the separatrix does not change significantly above the level of  $z \sim 1$  m, implying that the transition to the snowflake geometry would not have a significant direct effect on the core plasma. Despite the fact that the divertor plates in the snowflake case were situated at a very similar magnetic field, the change in the geometry has lead to

significant changes in the profile of plasma parameters near the divertor plates (with plasma parameters in the upper SOL being essentially the same); Fig. 8 illustrates this statement.

Addition of 1% of Argon (using the “fixed-fraction” model where the ratio of  $n_{Ar}/n_e$  is constant over the whole domain) gives rise to a significant reduction of the heat load on the outer divertor. In a typical case the heat load (in the presence of 1% of Ar) was roughly 2 times less in the snowflake case than in the standard case. The effect of the configuration on the heat flux on the inner divertor was less significant.

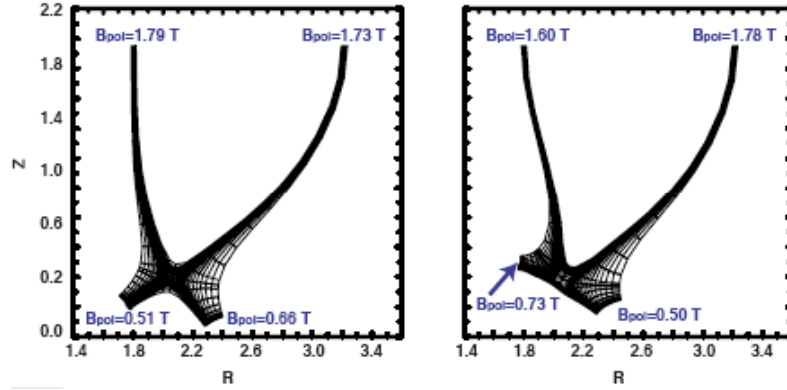


Fig. 7. Possible magnetic field structure for the FDF facility: standard X-point (left panel) and snowflake-plus (right panel). Values of  $B_{pol}$  in the midplane and at the divertor plate are indicated.

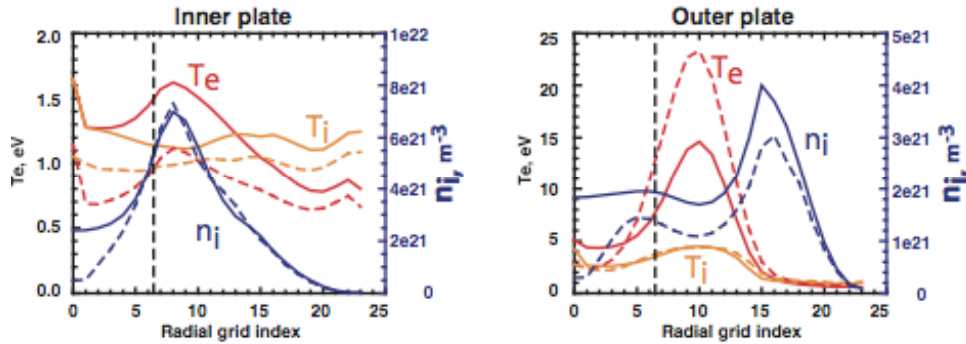


Fig. 8 UEDGE results for the FDF geometry. Solid lines – snowflake geometry; dashed lines – standard X-point geometry. Vertical dashed line marks the separatrix;  $n_i$  is the density of deuterium. There was no impurity radiation included for the shown case. Note a significant reduction of the electron temperature for the snowflake case.

## 5. Preventing divertor turbulence from propagating into main SOL

In the open field line region, the plasma pressure is typically small, and plasma turbulence is dominated by flute-like structures aligned with magnetic field lines. The dynamics of such structures is significantly affected by the presence of a magnetic field null and associated squeezing of the flux-tubes [12, 13]. In this section we describe squeezing in the snowflake geometry and find that it is much stronger than in the case of a standard X-point divertor.

Consider a flux tube whose cross-section is circular at some point in the divertor region (Fig. 9). Tracing this flux tube towards the vicinity of the null point and further to the main SOL, one finds that the cross-section is squeezed and becomes elliptic, very much as for a standard X-point divertor [12]. We denote the major and minor semi-axes of the flux-tube cross-section as  $w_{major}$  and  $w_{minor}$ . It is assumed that the cross-section is small enough that  $w_{major}$  does not exceed the length-scale of the magnetic field. As the flux through the cross-section remains the same along the length of the flux tube, and the field strength does not vary significantly, the product of the semi-axes remains constant, so that  $w_{minor} w_{major} = w_0^2$ .

One can conveniently characterize this stretching-squeezing effect by the parameter called “elongation”, the ratio of the long semi-axis to the initial radius,

$$E = w_{major} / w_0 > 1, \quad (5)$$

or, conversely,  $w_{minor} = w_0 / E$ . The elongation, as well as orientation of the axes of the ellipse, depends on the position along the flux-tube. The situation is illustrated in Fig. 9. Based on the results of Ref. [2], one can show that, for a flux tube circular at point “0”, the elongation at point “1” is:

$$E_1 \approx 1.57 \frac{l_D^2}{\Delta_0^2}, \quad (6)$$

where  $\Delta_0$  is the minimum distance of the magnetic surface to the x-point. This is significantly stronger elongation than for appearing in the standard X-point divertor [11]. The ellipse is tilted by an angle of approximately  $40^\circ$  with respect to the flux surface. If we continue to follow the flux tube further to the main SOL (point 2), the ellipse becomes more aligned with the flux surface, the elongation rapidly increases, and at the distance  $l_D$  above the null-point becomes  $E_2 \approx E_1^2$ .

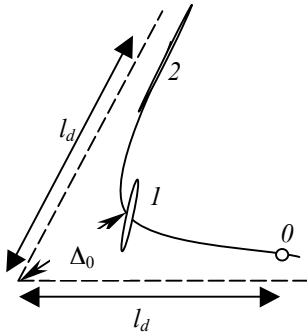


Fig.9. Flux-tube squeezing in a snowflake divertor.

The presence of the flux-tube squeezing prevents the divertor-leg turbulence from extending to the main SOL (this circumstance will be used in the next section). Indeed, even for a modest value of  $l_D=3\Delta_0$  the elongation  $E_2$  becomes  $\sim 150$ . This means that the perturbations, whose perpendicular scale-length in the divertor is as large as 100 ion gyro-radii, become squeezed to a size less than the ion gyro-radius as they are mapped to the main SOL. This, in turn, means that the plasma turbulence in the divertor is decoupled from that in the main SOL.

## 6. Recompression effects and the role of radiation

Reduction of the magnetic field in the strike point is a measure of the poloidal flux expansion and of the corresponding increase of the wetted area for a given SOL width. We measure the width in terms of the e-folding length  $\Delta_e$  of various quantities in the tokamak equatorial plane ( $\Delta_e$  may be different for these various quantities). The poloidal field flux through the SOL in the equatorial plane is  $2\pi B_{Pe} R \Delta_e$ . Assuming that the poloidal flux threading the SOL does not change between the midplane and divertor (possible deviations from this assumptions are considered later in this section), one finds the wetted area on the divertor plate,  $(2\pi R \Delta_e) B_{Pe} / B_{PD}$ . Obviously, the surface area is larger for a weaker poloidal field at the strike point (Cf. Sec. 2).

Further increase of the wetted area can be achieved by tilting the divertor surface so as to make the angle  $\alpha$  between the poloidal magnetic field and divertor surface small (Fig. 10). This, obviously, yields additional large factor  $1/\sin\alpha$  in the wetted surface area:

$$S_w = 2\pi R \Delta_e B_{Pe} / (B_{PD} \sin\alpha). \quad (7)$$

However, this approach has its limits, associated with engineering constraints. What may actually be a limitation is the angle between the full magnetic field vector and the surface [14]. As the poloidal field  $B_{PD}$  at the divertor plate is small compared to the toroidal field,  $B_{TD}$ , the angle  $\gamma$  between the surface and the full vector is

$$\gamma \approx B_{PD} \sin\alpha / B_{TD} \ll \alpha. \quad (8)$$

Possible imperfections in the alignment should be compared with this angle, not  $\alpha$ . Thus, it is obvious that that the wetted area  $S_W = 2\pi R \Delta_e B_{Pe} / (B_{PD} \sin \alpha)$  is limited to

$$S_W < 2\pi R \Delta_e B_{Pe} / (B_{TD} \gamma_{\min}). \quad (9)$$

Remarkably,  $S_W$  does not depend on the poloidal field at the strike point ( $B_{PD}$ ).

This result suggests the following approach: use a strong flux expansion in the vicinity of the null-point to radiate a maximum possible power, and then tilt the divertor plate in the recompression zone, as shown in Fig. 10, to reach the largest-possible wetted area (9). The use of relatively long divertor “legs”, with  $l_D$  (Fig. 10) large compared to the size of the expansion zone  $\Delta_0$  near the null-point opens up the possibility of further spreading of the plasma flow by virtue of enhanced turbulence in the divertor legs [13]. The turbulence is sensitive to the tilt angle  $\alpha$  and can be enhanced for small  $\alpha$ .

The turbulence induced in the divertor legs does not penetrate to the main SOL because of the strong squeezing of the flux-tubes passing near the magnetic null (Sec. 5). Therefore, the enhanced divertor-leg turbulence does not lead to degradation of the confinement of the core plasma. Note that, under realistic conditions, the length of the divertor legs is significantly smaller than the distance from midplane to the null-point. Accordingly, parallel convection/conduction of heat in the divertor takes less time than in the main SOL. Therefore, in order to produce strong plasma expansion in the divertor leg, cross-field transport should be much stronger here than in the main SOL. But the two regions are decoupled from each other (see Sec. 5), and significant difference in transport coefficients may be possible.

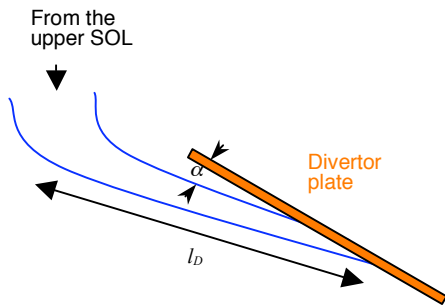


*Fig. 10 The geometry of a “long-legged” snowflake divertor (the outer leg). Only part of the divertor plate is shown (the one containing wetted area). Other material surfaces used as baffles, limiters, etc are not drawn. Shown in blue are two flux surfaces. The major axis is to the left.*

In order to further reduce heat flux at the divertor targets, one can consider increasing the radiated power near the divertor target surfaces [15] by puffing impurities directly into the “closed” divertor; the escape of the impurity ions into the main plasma would be inhibited by the enhancing the flow of deuterium toward the divertor plates, e.g., “puff-and-pump.” We leave detailed assessment of this scenario for future work.

## 7. Discussion

We have provided a brief discussion of the properties of a snowflake divertor. The set of coils required to generate the snowflake configuration is quite simple. The distance from the coils to the magnetic null is large, thereby allowing placement of the coils outside toroidal field coils. The snowflake-plus configuration allows one to combine the robustness of the standard X-point configuration and large flux expansion typical of the snowflake geometry. It is quite robust with respect to possible uncontrolled variations of the plasma current.

In addition to the obvious effect on the flux expansion near the null point (typically, by a factor of 2-3 compared to the standard X-point configuration), the snowflake divertor provides additional degree of control over a variety of processes in the scrape-off-layer and in the pedestal region. In particular, the snowflake allows one to control the magnetic shear in the pedestal region just inside the separatrix, thereby providing a tool for affecting ELM

activity. The snowflake leads to a stronger squeezing of the magnetic flux-tubes passing near the magnetic null point, thereby affecting divertor-leg instabilities and instabilities in the vicinity of the null-point.

Because of a strong flux expansion, the snowflake increases the SOL volume. Therefore, it holds promise for improved operation in the radiative mode. If divertor legs are long enough, one can try to increase divertor cross-field transport and induce additional spreading of the plasma in the divertor area.

## Acknowledgments

Prepared by LLNL under Contract DE-AC52-07NA27344; research at GA was supported by U.S. DoE contract DE-FC02-04ER-54698; research at PPPL was supported by U.S. DOE contract DE-AC02-76-CH03073.

## References

1. D.D. Ryutov. Phys. Plasmas, **14**, 064502 (2007); Erratum: Phys. Plasmas, **15**, 069901 (2008); D.D. Ryutov. Paper D1.002, 34<sup>th</sup> EPS Conf. on Plasma Phys, Warsaw, 2007 (<http://epsppd.epfl.ch/Warsaw/start.htm>).
2. D.D. Ryutov, R.H. Cohen, T.D. Rognlien, M.V. Umansky. Phys. Plasmas, **15**, 092501 (2008).
3. M. Kotschenreuther, P.M. Valanju, S.M. Mahajan, J.C. Wiley. Phys. Plasmas, **14**, 072502 (2007).
4. M. Kotschenreuther, P.M. Valanju, S.M. Mahajan. "High Power Density Experiment (HDPX) – A Next Step Device in the Age of ITER." Paper 1C presented at the 2008 Intern. Fusion Theory Conf, Boulder, CO, March 31-April 2, 2008.
5. P.B. Snyder, H.R. Wilson, J.R. Ferron, L.L. Lao, A.W. Leonard, T.H. Osborne, A.D. Turnbull, D. Mossessian, M. Murakami, X.Q. Xu. Phys. Plasmas, **9**, 2037 (2002)
6. A.J. Webster, C.G. Gimblett. "The Ideal Magnetohydrodynamic Peeling Mode Instability," Paper 3B03, International Sherwood Fusion Theory Conference, Boulder, CO, 31 March – 2 April 2008; A.J. Webster, C.G. Gimblett. 34<sup>th</sup> EPS Conference on Plasma Phys. Warsaw, 2-6 July 2007, ECA Vol. 31F, P-4.088.
7. L.D. Pearlstein, R.H. Bulmer, T.A. Casper, E.B. Hooper, R.A. Jong, T.B. Kaiser, L.L. LoDestro, H.L. Berk, "Predictive Modeling of Axisymmetric Toroidal Configurations," Proc. of the 28th EPS (June, 2001), Funchal, Madeira, and references therein.
8. R.J. Goldston, J. Menard, J.P. Allain, J.N. Brooks, et al. Poster GP6.00125, 50th Annual Meeting of the Division of Plasma Physics, November 17–21, 2008, Dallas, Texas.
9. J. Menard. ISOLVER code, PPPL.
10. R.D. Stambaugh, V.S. Chan, A.M. Garofalo, J.P. Smith, C.P.C. Wong, Poster TP6.00049; A.M. Garofalo T.W. Petrie, J.P. Smith, M.R. Wade, et al. Poster TP6.00051; 50th Annual Meeting of the Division of Plasma Physics, November 17–21, 2008 Dallas, Texas.;
11. T.D. Rognlien J.L. Milovich, M.E. Rensink, G.D. Porter. J. Nucl. Mat., **196-198**; 347 (1992).
12. D.Farina, R.Pozzoli, D.D. Ryutov. Nuclear Fusion, **33**, 1315 (1993).
13. R.H. Cohen, B. LaBombard, L.L. LoDestro, T.D. Rognlien, D.D. Ryutov, J.L. Terry, M.V. Umansky, X.Q. Xu, S. Zweben. Nucl. Fusion, **47**, 612 (2007).
14. A.S. Kukushkin. Private comm. to D.D. Ryutov, July 2007.
15. T.W. Petrie, M.R. Wade, N.H. Brooks, M.E. Fenstermacher et al. J. of Nucl. Mat., **363-365**, 416 (2007).